J|A|C|S
ARTICLES
Published on Web 03/13/2007

An Enzymatically Activated Fluorescence Probe for Targeted Tumor Imaging

Mako Kamiya,[†,‡] Hisataka Kobayashi,*[,§] Yukihiro Hama,[§] Yoshinori Koyama,[§] Marcelino Bernardo,[||] Tetsuo Nagano,[†,‡] Peter L. Choyke,[§] and Yasuteru Urano*[,†,⊥]

Contribution from the Graduate School of Pharmaceutical Sciences, The University of Tokyo, 7-3-1 Hongo, Bunkyo-ku, Tokyo 113-0033, Japan, CREST, Japan Science and Technology Agency, 4-1-8 Honcho, Kawaguchi, Saitama 332-0012, Japan, Molecular Imaging Program, Center for Cancer Research, National Cancer Institute, National Institutes of Health, Bldg. 10, Rm. 1B40, 10 Center Drive, Bethesda, Maryland 20892-1088, Research Technology Program, Science Applications International Corporation (SAIC)-Frederick, Frederick, Maryland 21702, and PRESTO, Japan Science and Technology Agency, 4-1-8 Honcho, Kawaguchi, Saitama 332-0012, Japan

Received October 28, 2006; E-mail: kobayash@mail.nih.gov; urano@mol.f.u-tokyo.ac.jp

Abstract: β-Galactosidase is a widely used reporter enzyme, but although several substrates are available for *in vitro* detection, its application for *in vivo* optical imaging remains a challenge. To obtain a probe suitable for *in vivo* use, we modified our previously developed activatable fluorescence probe, TG-βGal (*J. Am. Chem. Soc.* **2005**, *127*, 4888−4894), on the basis of photochemical and photophysical experiments. The new probe, **AM-TG-βGal**, provides a dramatic fluorescence enhancement upon reaction with β-galactosidase, and further hydrolysis of the ester moiety by ubiquitous intracellular esterases affords a hydrophilic product that is well retained within the cells without loss of fluorescence. We used a mouse tumor model to assess the practical utility of **AM-TG-βGal**, after confirming that tumors in the model could be labeled with an avidin-β-galactosidase conjugate. This conjugate was administered to the mice *in vivo*, followed by **AM-TG-βGal**, and subsequent *ex vivo* fluorescence imaging clearly visualized intraperitoneal tumors as small as 200 μm. This strategy has potential clinical application, for example, in video-assisted laparoscopic tumor resection.

Introduction

Marker enzymes are widely used to identify cell types or specific haptens, to examine transcription regulation or to evaluate the efficiency of transfection experiments. *Escherichia coli* β-galactosidase is well characterized and extensively used as a marker enzyme in enzyme-linked immunosorbent assays (ELISA),[1−3] *in situ* hybridizations,[4−6] classification of mycobacteria,[7] and gene expression studies.[8−11] This enzyme is especially useful for studying gene expression because of its stability, high turnover rate, and ease of conjugation and detection, as well as the absence of endogenous β-galactosidase activity in eukaryotic cells. A range of substrates has been developed including colorimetric,[12,13] fluororescence,[14−19] chemiluminescence,[20,21] and paramagnetic probes,[22] though they have mostly been used in *in vitro* systems, with only a few successful applications *in vivo*.[23−25]

† The University of Tokyo.
‡ CREST, JST Agency.
§ NCI, NIH.
|| SAIC-Frederick.
⊥ PRESTO, JST Agency.

(1) Konijn, A. M.; Levy, R.; Link, G.; Hershko, C. J. *Immunol. Methods* **1982**, *54*, 297−307.
(2) Armenta, R.; Tarnowski, T.; Gibbons, I.; Ullman, E. F. *Anal. Biochem.* **1985**, *146*, 211−219.
(3) Baruch, D.; Glickstein, H.; Cabantchik, Z. I. *Exp. Parasitol.* **1991**, *73*, 440−450.
(4) Fields, S.; Song, O. K. *Nature* **1989**, *340*, 245−246.
(5) Vidal, M.; Brachmann, R. K.; Fattaey, A.; Harlow, E.; Boeke, J. D. *Proc. Natl. Acad. Sci. U.S.A.* **1996**, *93*, 10315−10320.
(6) Fields, S.; Sternglanz, R. *Trends Genet.* **1994**, *10*, 286−292.
(7) Hamid, M. E.; Chun, J.; Magee, J. G.; Minnikin, D. E.; Goodfellow, M. *Zentralbl Bakteriol.* **1994**, *280*, 476−87.
(8) Nolan, G. P.; Fiering, S.; Nicolas, J.-F.; Herzenberg, L. A. *Proc. Natl. Acad. Sci. U.S.A.* **1988**, *85*, 2603−2607.
(9) Fiering, S.; Roederer, M.; Nolan, G. P.; Micklem, D. R.; Parks, D. R.; Herzenberg, L. A. *Cytometry* **1991**, *12*, 291−301.
(10) Berger, C. N.; Tan, S.-S.; Sturm, K. S. *Cytometry* **1994**, *17*, 216−223.
(11) Lin, S.; Yang, S.; Hopkins, N. *Dev. Biol.* **1994**, *161*, 77−83.
(12) Sanes, J. R.; Rubenstein, J. L.; and Nicolas, J. F. *EMBO J.* **1986**, *5*, 3133−3142.
(13) James, A. L.; Perry, J. D.; Chilvers, K.; Robson, I. S.; Armstrong, L.; Orr, K. E. *Lett. Appl. Microbiol.* **2000**, *30*, 336−340.
(14) Rotman, B.; Zderic, J. A.; Edelstein, M. *Proc. Natl. Acad. Sci. U.S.A.* **1963**, *50*, 1−6.
(15) Rakhmanova, V. A.; MacDonald, R. C. *Anal. Biochem.* **1998**, *257*, 234−237.
(16) Young, D. C.; Kingsley, S. D.; Ryan, K. A.; Dutko, F. J. *Anal. Biochem.* **1993**, *215*, 24−30.
(17) Chilvers, K. F.; Perry, J. D.; James, A. L.; Reed, R. H. *J. Appl. Microbiol.* **2001**, *91*, 1118−1130.
(18) Gee, K. R.; Sun, W. C.; Bhalgat, M. K.; Upson, R. H.; Klaubert, D. H.; Latham, K. A.; Haugland, R. P. *Anal. Biochem.* **1999**, *273*, 41−48.
(19) Corey, P. F.; Trimmer, R. W.; Biddlecom, W. G. *Angew. Chem., Int. Ed. Engl.* **1991**, *30*, 1646−1648.
(20) Takayasu, S.; Maeda, M.; Tsuji, A. *J. Immunol. Methods* **1985**, *83*, 317−325.
(21) Arakawa, H.; Maeda, M.; Tsuji, A. *Anal. Biochem.* **1991**, *199*, 238−42.
(22) Alauddin, M. M.; Louie, A. Y.; Shahinian, A.; Meade, T. J.; Conti, P. S. *Nucl. Med. Biol.* **2003**, *30*, 261−265.
(23) Tung, C.-H.; Zeng, Q.; Shah, K.; Kim, D.-E.; Schellingerhout, D.; Weissleder, R. *Cancer Res.* **2004**, *64*, 1579−1583.

10.1021/ja067710a CCC: $37.00

Scheme 1. Reaction Schemes of Our Fluorescence Probes with β-Galactosidase and Intracellular Esterase[a]

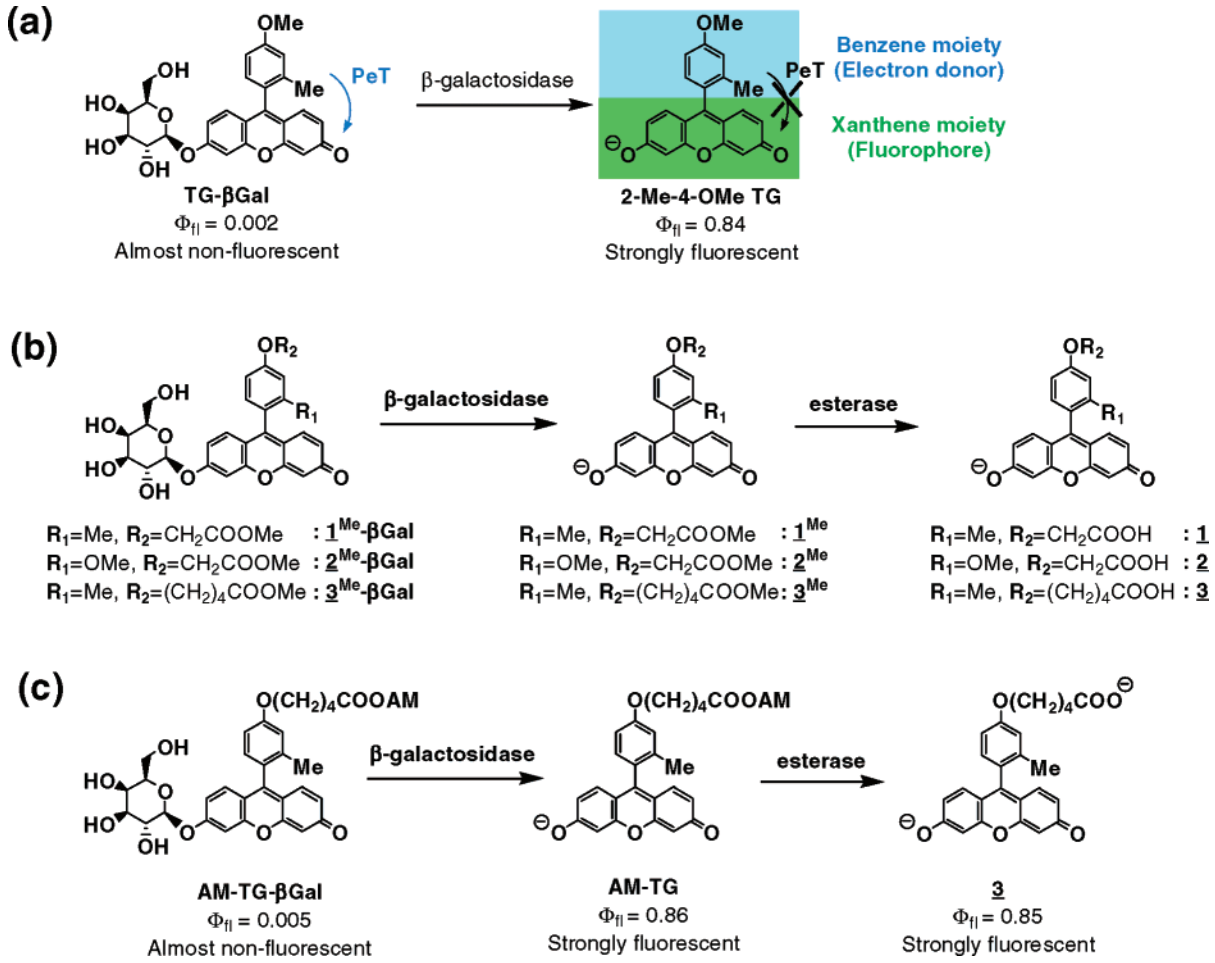

[a] (a) Reaction of our previously reported β-galactosidase probe, TG-βGal, with β-galactosidase. (b) Newly developed β-galactosidase substrates bearing an esterase-sensitive methylester, **1**^{Me}-β**Gal**, **2**^{Me}-β**Gal**, and **3**^{Me}-β**Gal**. (c) Our newly developed fluorescence probe, **AM-TG-**β**Gal**, which shows a large fluorescence increase upon reaction with β-galactosidase and is further hydrolyzed by intracellular esterase to the free carboxylate, which is well retained in the cells without loss of fluorescence.

In our previous work, we focused on simple, rapid, and sensitive detection of β-galactosidase activity and developed a highly sensitive fluorescence probe for β-galactosidase, TG-βGal (Scheme 1a).[26] This probe was rationally designed to show a dramatic fluorescence activation (up to 440-fold) upon reaction with β-galactosidase and was successfully used to visualize β-galactosidase activity in living cells. We considered that such probes might be suitable to visualize tumors *in vivo*. For example, in the clinical field, video-assisted laparoscopic surgery is becoming one of the standard methods for resecting metastases,[27] and it already relies on optical cameras that could easily be adapted to employ fluorescence imaging.[28] Probes such as TG-βGal have appropriate characteristics (high molar extinction coefficient and high fluorescence quantum yield (Φ_{fl}) in aqueous media after reaction with the target enzymes) for visualization of surface tumors such as intraperitoneal tumors, for which brightness of the fluorophores is more important than long-wavelength excitability, as the light does not need to penetrate the skin and tissues. Our aim in the present work was to design a TG-βGal-based probe that would be suitable for *in vivo* tumor imaging and to test its suitability for this purpose in an animal tumor model. TG-βGal itself was unsuitable, as its hydrophobic fluorescent hydrolysis product is easily washed out from cells (Figure 1a). We therefore designed and synthesized a new probe, **AM-TG-**β**Gal**. Like TG-βGal, **AM-TG-**β**Gal** shows a dramatic fluorescence enhancement upon hydrolysis with β-galactosidase. Further, the ester moiety of its hydrolysis product, **AM-TG**, is cleaved by ubiquitous intracellular esterases, generating a hydrophilic product that is well retained within the cells without loss of fluorescence. To examine whether **AM-TG-**β**Gal** would indeed be suitable for *in vivo* tumor imaging, we used the following two-step strategy in a mouse tumor model. First, an avidin-β-galactosidase conjugate was administered to the mice to target the enzyme to tumors, and then **AM-TG-**β**Gal** was administered. Subsequent *ex vivo* fluorescence imaging clearly visualized intraperitoneal tumors as small as 200 μm. Our findings demonstrate the

(24) Louie, A. Y.; Hüber, M. M.; Ahrens, E. T.; Rothbächer, U.; Moats, R.; Jacobs, R. E.; Fraser, S. E.; Meade, T. J. *Nat. Biotechnol.* **2000**, *18*, 321−325.
(25) Wehrman, T. S.; von Degenfeld, G.; Krutzik, P. O.; Nolan, G. P.; Blau, H. M. *Nat. Methods* **2006**, *3*, 295−301.
(26) Urano, Y.; Kamiya, M.; Kanda, K.; Ueno, T.; Hirose, K.; Nagano, T. *J. Am. Chem. Soc.* **2005**, *127*, 4888−4894.
(27) Takeda, A.; Manabe, S.; Mitsui, T.; Nakamura, H. *Gynecol. Surg.* **2006**, *3*, 45−48.
(28) Kim, S.; Lim, Y. T.; Soltesz, E. G.; De Grand, A. M.; Lee, J.; Nakayama, A.; Parker, J. A.; Mihaljevic, T.; Laurence, R. G.; Dor, D. M.; Cohn, L. H.; Bawendi, M. G.; Frangioni, J. V. *Nat. Biotechnol.* **2004**, *22*, 93−97.

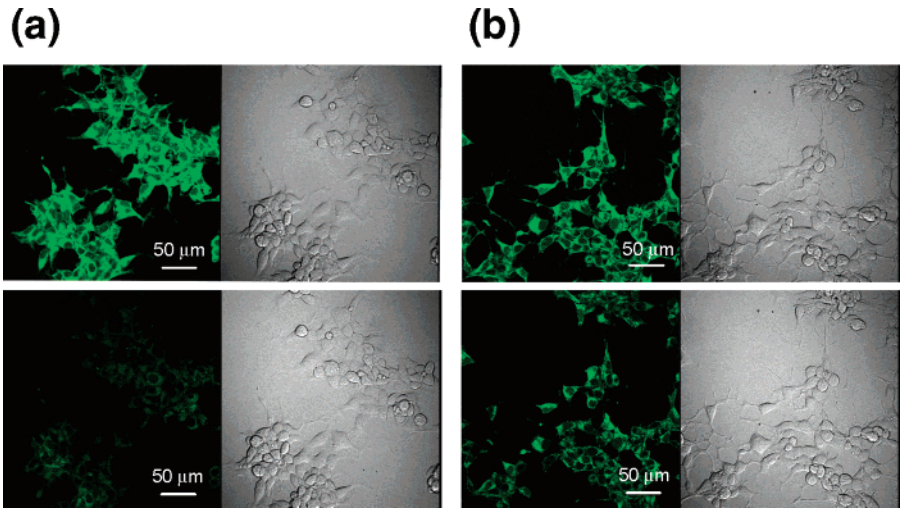

Figure 1. Fluorescence microscopic imaging of β-galactosidase activity in living cells with TG-βGal and **AM-TG-βGal** and comparison of their intracellular retention. HEK293 cells expressing β-galactosidase were incubated with a 10 μM solution of TG-βGal (a) or AM-TG-βGal (b) in physiological salt solution, pH 7.4, containing 150 mM NaCl, 4 mM KCl, 2 mM $CaCl_2$, 1 mM $MgCl_2$, 5 mM HEPES, and 0.1% glucose (PSS), and 0.1% DMSO as a cosolvent for 2 h. Then, confocal fluorescence images and DIC images were captured before (Upper) and after (Lower) washing with PSS. A clear decrease of fluorescence was observed in the case of cells incubated with TG-βGal, while little change was observed in the case of cells incubated with **AM-TG-βGal**.

Scheme 2. Synthetic Scheme of $\underline{1}^{Me}$-β**Gal**[a]

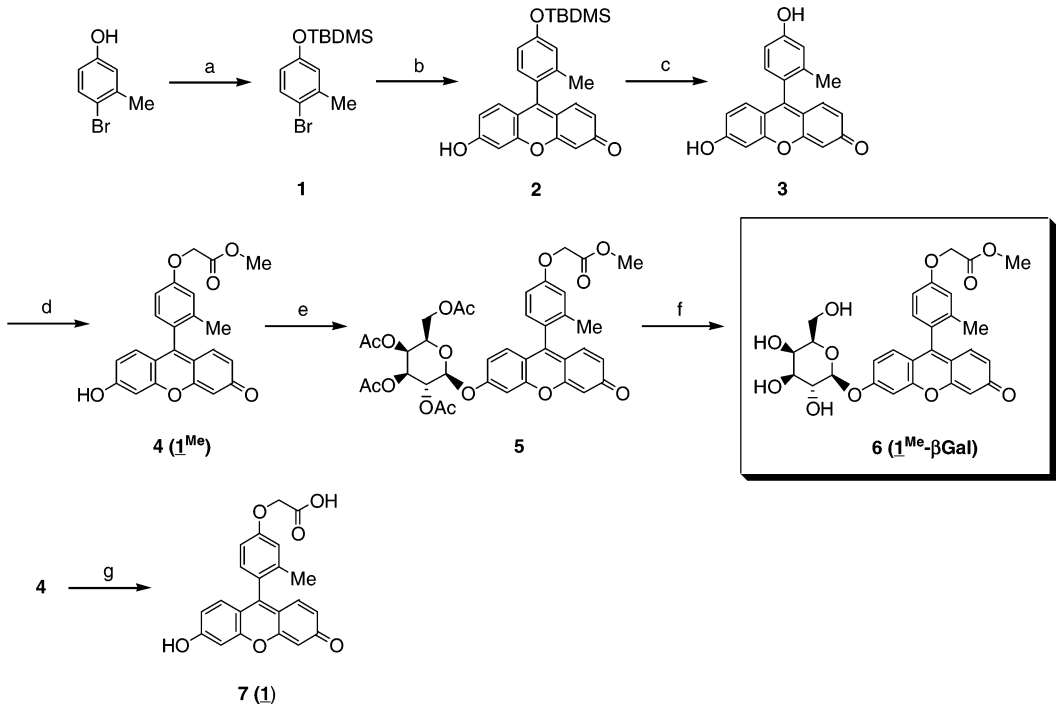

[a] Reagents: (a) TBDMS−Cl, imidazole, DMF; (b) 3,6-bis(*tert*-butyldimethylsilanyloxy)xanthen-9-one, *t*-BuLi, THF; (c) TBAF, THF; (d) methyl bromoacetate, Cs_2CO_3, DMF; (e) 2,3,4,6-tetra-*O*-acetyl-α-D-galactopyranosyl bromide, Cs_2CO_3, DMF; (f) NaOMe, MeOH; (g) aq. NaOH, MeOH.

feasibility of this approach to tumor imaging, which we believe has potential clinical applicability, for example in video-assisted laparoscopic tumor resection.

Results and Discussion

Design and Synthesis of New Probes with Improved Cellular Retention. We aimed to modify TG-βGal to obtain sufficient intracellular retention in the living cells by adopting the strategy of introducing an acetoxymethyl (AM) ester group.[29,30] We anticipated that the AM-derivatized β-galactosidase probe would be hydrolyzed both by β-galactosidase to show large fluorescence activation and by ubiquitous intracellular esterases to yield the hydrophilic fluorophore with a free carboxylate group, which would not readily leak from the cells.

From the synthetic point of view, we first thought it would be simple to introduce a methoxycarbonyl methoxy group instead of the methoxy group of TG-βGal. According to Scheme 2, we synthesized $\underline{1}^{Me}$-β**Gal**. Although $\underline{1}^{Me}$ (the hydrolysis product of $\underline{1}^{Me}$-β**Gal**) is highly fluorescent ($\Phi_{fl} = 0.85$), $\underline{1}^{Me}$-

(29) Minta, A.; Kao, J. P. Y.; Tsien, R. Y. *J. Biol. Chem.* **1989**, *264*, 8171−8178.

(30) Zlokarnik, G.; Negulescu, P. A.; Knapp, T. E.; Mere, L.; Burres, N.; Feng, L.; Whitney, M.; Roemer, K.; Tsien, R. Y. *Science* **1998**, *279*, 84−88.

Table 1. Absorption and Fluorescence Properties of the Newly Developed β-Galactosidase Substrates and their Esterase and/or β-Galactosidase-Catalyzed Hydrolysis Products

compound	absorption maximum[a] (nm)	emission maximum[a] (nm)	fluorescence quantum yield[b]	fluorescence enhancement[c]
1^{Me}-βGal	454	515	0.069	46
2^{Me}-βGal	452	527	0.004	410
3^{Me}-βGal	452	512	0.009	370
AM-TG-βGal	453	518	0.005	470
1^{Me}	492	511	0.85	-
1	491	510	0.83	-
2^{Me}	494	516	0.67	-
2	494	515	0.32	-
3^{Me}	491	510	0.85	-
3	491	510	0.85	-
AM-TG	491	510	0.86	-

[a] Data for **1^{Me}-βGal**, **2^{Me}-βGal**, **3^{Me}-βGal**, and **AM-TG-βGal** were measured in 100 mM sodium phosphate buffer, pH 7.4, containing 0.1% DMSO as a cosolvent. Data for **1^{Me}**, **2^{Me}**, **3^{Me}**, **1**, **2**, **3**, and **AM-TG** were measured in 100 mM sodium phosphate buffer, pH 9.0, containing 0.1% DMSO as a cosolvent. [b] For determination of the fluorescence quantum yield, fluorescein in 100 mM aq. NaOH (0.85) was used as a fluorescence standard.[39] [c] Fluorescence enhancement represents the ratio of fluorescence intensity at 509−511 nm before and after hydrolysis by β-galactosidase.

βGal had a relatively high background fluorescence (Φ_{fl} = 0.069), so the fluorescence enhancement after activation was relatively modest (46-fold) (Table 1, Scheme 1b).

In order to understand this result, we have to consider the mechanism underlying the fluorescence off/on switching of TG-βGal, i.e., intramolecular photoinduced electron transfer (PeT), which is a nonradiative pathway from the excited-state of the fluorophore. As we demonstrated in our previous paper, fluorescein derivatives, including TokyoGreens, can be considered to consist of two functional components from the viewpoint of fluorescence, namely a benzene moiety which is the electron donor and a xanthene moiety which is the fluorophore (Scheme 1a).[31,32] Moreover, the oxidation potential of the benzene moiety can greatly influence the efficiency of PeT, and *m*-methoxytoluene, the benzene moiety of TG-βGal, has the most suitable oxidation potential as an electron donor (1.66 V vs SCE, Table 2) in order to convert the change in reduction potential of the xanthene moiety induced by β-galactosidase-assisted hydrolysis to the maximal change in fluorescence intensity.[26] Therefore, we measured the oxidation potential of *m*-methoxycarbonylmethoxytoluene, the benzene moiety of **1^{Me}-βGal** (**Bn(1^{Me})**), and found that the oxidation potential had been altered to a higher value (1.77 V vs SCE, Table 2) by the introduction of the electron-withdrawing methoxycarbonyl group with a short methylene linker, and this accounted for the increase of the background fluorescence of **1^{Me}-βGal**. The calculated energy level of the highest occupied molecular orbital (HOMO), which is known to be linearly correlated with measured oxidation potential, supported this view (−0.2141 hartree for *m*-methoxytoluene and −0.2207 hartree for **Bn(1^{Me})**) (Table 2).

Thus, we employed a strategy to lower the oxidation potential of **Bn(1^{Me})** to a value similar to that of *m*-methoxytoluene (1.66 V vs SCE) by introducing an electron-donating group. The oxidation potential of *m*-methoxycarbonylmethoxyanisole (**Bn(2^{Me})**), in which the methyl group of **Bn(1^{Me})** is replaced with a methoxy group, proved to be sufficiently small to suppress the background fluorescence (1.57 V vs SCE, Table 2) via the PeT pathway. Thus, we designed and synthesized **2^{Me}-βGal** according to Scheme 3. As we expected, **2^{Me}-βGal** showed low background fluorescence (Φ_{fl} = 0.004), whereas **2^{Me}** (the hydrolysis product of **2^{Me}-βGal**) showed strong fluorescence (Φ_{fl} = 0.67) (Table 1). Thus, the fluorescence enhancement is 410-fold. Unfortunately, however, the fluorescence intensity of **2^{Me}** was altered by esterase activity, because hydrolysis of the ester group lowered the oxidation potential too much, which led to quenching of the fluorescence output of **2** (Φ_{fl} = 0.32), the final fluorescent species generated from **2^{Me}-βGal** (Scheme 1b, Table 1, Figure 2). For the reliable fluorescence detection of β-galactosidase activity, the fluorescence should be unaffected by cleavage of the ester.

The solution we adopted was to reduce the electron-withdrawing effect of the methoxycarbonyl group of **Bn(1^{Me})** by lengthening the methylene chain between the methoxycarbonyl group and the benzene moiety. We calculated the HOMO energy levels of the benzene moiety with various lengths of methylene chain at the B3LYP/6-31G level and predicted that a HOMO level similar to that of *m*-methoxytoluene could be achieved by inserting three or four methylene units between the methoxycarbonyl group and the benzene moiety (Table 2). Oxidation potentials of *m*-methoxycarbonylbutyloxytoluene (**Bn(3^{Me})**) measured by cyclic voltammetry were consistent with this expectation (1.62 V vs SCE, Table 2). According to Scheme 4, we synthesized **3^{Me}-βGal** with four methylene units. The background fluorescence of **3^{Me}-βGal** was successfully suppressed (Φ_{fl} = 0.009), while the hydrolysis product of **3^{Me}-βGal** (**3^{Me}**) emits sufficiently strong fluorescence (Φ_{fl} = 0.85) (Scheme 1b, Table 1). The fluorescence enhancement ratio that can be obtained with **3^{Me}-βGal** is approximately 360-fold. Moreover, its fluorescence was independent of the esterase activity (Φ_{fl} of **3** was 0.85, Figure 2). Therefore, we derivatized **3^{Me}-βGal** to the AM ester, which was designated **AM-TG-βGal** (Scheme 5). As expected, **AM-TG-βGal** shows almost no fluorescence (Φ_{fl} = 0.005) but is converted by β-galactosidase to highly fluorescent **AM-TG** (Φ_{fl} = 0.86), affording a 470-fold fluorescent enhancement (Scheme 1c, Table 1, Figure 3). Thus, we finally succeeded in developing a highly sensitive fluorescence probe for β-galactosidase with an esterase-sensitive moiety that could be removed without loss of the strong fluorescence, by finely tuning the oxidation potential to retain the highly activatable character of TG-βGal.

Relationship between Oxidation Potential and Fluorescence Quantum Yield. We plotted the fluorescence quantum yields of the anionic and neutral forms of **1^{Me}**, **2^{Me}**, and **3^{Me}** (the scaffold fluorophores of **1^{Me}-βGal**, **2^{Me}-βGal**, and **3^{Me}-βGal**) on a graph showing the relationship between the oxidation potential and fluorescence quantum yield (Φ_{fl}) of previously reported TokyoGreen derivatives (Figure 4, Table 3).[26] All the values including that of **1^{Me}**, **2^{Me}**, and **3^{Me}** can be fitted with the Marcus equation. It can be seen that **3^{Me}** lies between the fluorescence off/on thresholds of the anionic and neutral forms, indicating that it is the most suitable scaffold fluorophore for developing a highly sensitive fluorescence probe with enhanced cellular retention. This result also confirms that the previously reported design strategy is valid for developing new probes with desirable features.

(31) Tanaka, K.; Miura, T.; Umezawa, N.; Urano, Y.; Kikuchi, K.; Higuchi, T.; Nagano, T. *J. Am. Chem. Soc.* **2001**, *123*, 2530−2536.
(32) Miura, T.; Urano, Y.; Tanaka, K.; Nagano, T.; Ohkubo, K.; Fukuzumi, S. *J. Am. Chem. Soc.* **2003**, *125*, 8666−8671.

Table 2. Oxidation Potential and Calculated HOMO Energy Level of the Benzene Moiety of **1^{Me}-βGal**, **2^{Me} βGal**, and **3^{Me}-βGal**; **Bn(1^{Me})**, **Bn(2^{Me})**, and **Bn(3^{Me})**

Benzene moiety		Oxidation potential (V vs SCE)[a]	Calcd. HOMO (hartrees)[b]
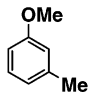	*m*-methoxytoluene	1.66	-0.2141
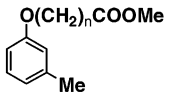	n = 1: **Bn(1^{Me})**	1.77	-0.2207
	n = 2:	n.d.[c]	-0.2198
	n = 3:	n.d.[c]	-0.2156
	n = 4: **Bn(3^{Me})**	1.62	-0.2152
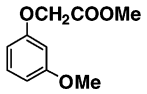	**Bn(2^{Me})**	1.57	-0.2107

[a] All data were measured in 100 mM TBAF MeCN, with Ag/Ag^+ as a reference electrode. [b] HOMO energy level was calculated at the B3LYP/6-31G level. [c] n.d.; not determined.

Scheme 3. Synthetic Scheme of **2^{Me}-βGal**[a]

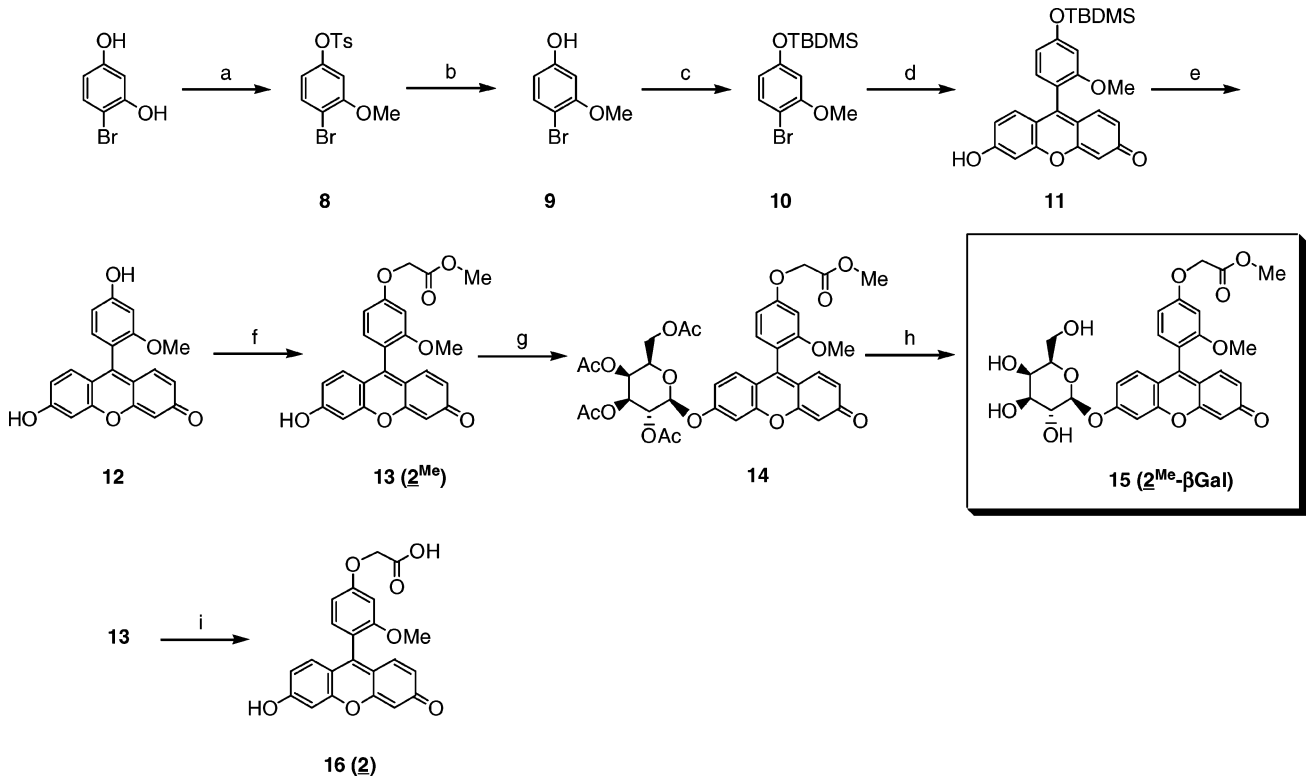

[a] Reagents. (a) (1) TsCl, K_2CO_3, acetone, (2) MeI; (b) aq. NaOH, MeOH; (c) TBDMS−Cl, imidazole, DMF; (d) 3,6-bis(*tert*-butyldimethylsilanyloxy)xanthen-9-one, *t*-BuLi, THF; (e) TBAF, THF; (f) methyl bromoacetate, Cs_2CO_3, DMF; (g) 2,3,4,6-tetra-*O*-acetyl-α-D-galactopyranosyl bromide, Cs_2CO_3, DMF; (h) NaOMe, MeOH; (i) aq. NaOH, MeOH.

Cellular Retention. We next examined whether or not the newly developed **AM-TG-βGal** is better retained in living cells as compared with TG-βGal. HEK293 cells expressing β-galactosidase were incubated with 10 μM **AM-TG-βGal**, and fluorescence images were captured before and after the washing of the cells (Figure 1b). As expected, washing caused little change in the fluorescence, in contrast with the case of TG-βGal. This difference can be explained in terms of superior retention of the ultimate hydrolysis product of **AM-TG-βGal** in the living cells.

Targeting of β-Galactosidase to Tumor Cells. We next tried to apply **AM-TG-βGal** to visualize intraperitoneal tumors in mice. For this purpose, we adopted a two-step procedure, employing a tumor-targeting avidin-β-galactosidase conjugate (avidin-β-galactosidase) to localize β-galactosidase to cancer cells *in vivo*,[33,34] followed by the administration of **AM-TG-**

Scheme 4. Synthetic Scheme of **3^{Me}-βGal**[a]

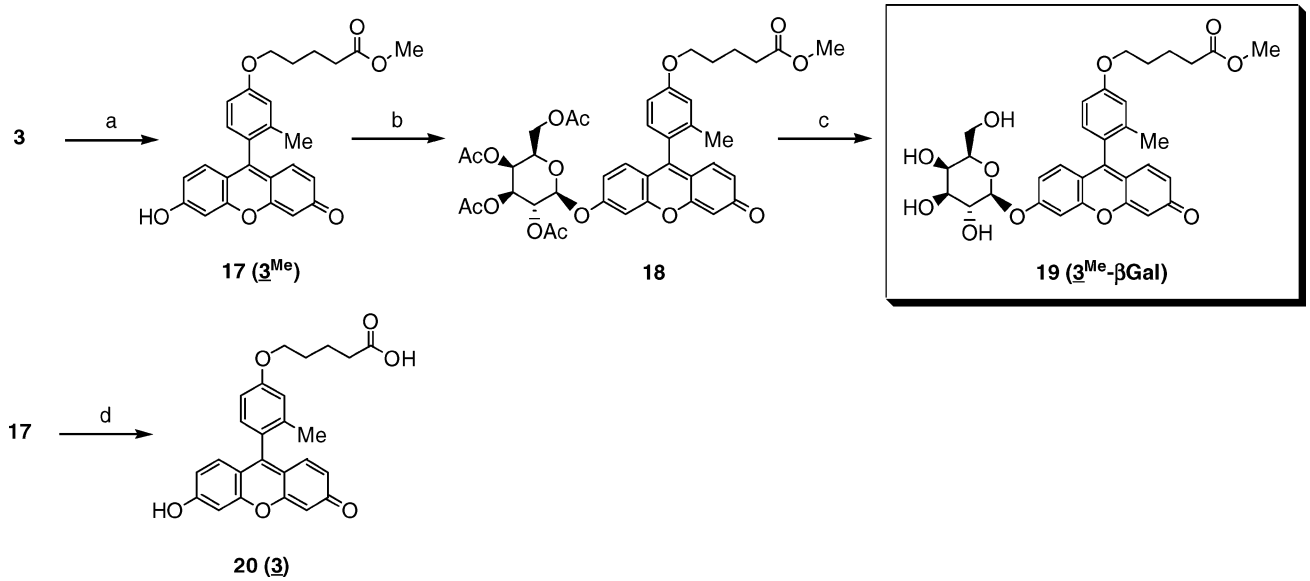

[a] Reagents: (a) methyl bromovalerate, Cs_2CO_3, DMF; (b) 2,3,4,6-tetra-*O*-acetyl-α-D-galactopyranosyl bromide, Cs_2CO_3, DMF; (c) NaOMe, MeOH; (d) aq. NaOH, MeOH.

Scheme 5. Synthetic Scheme of **AM-TG-βGal**[a]

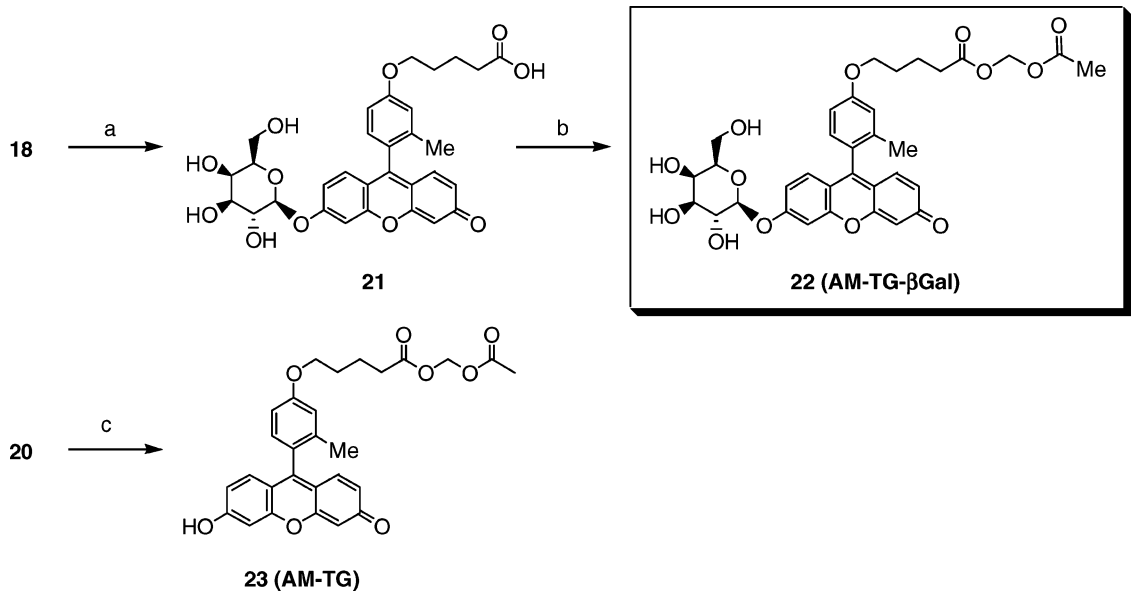

[a] Reagents: (a) aq. NaOH, MeOH/H_2O; (b) bromomethyl acetate, DIEA, MeOH/MeCN; (c) bromomethyl acetate, DIEA, DMF.

βGal. Avidin was chosen based on its high affinity for lectins on the surface of several human ovarian cancer cell lines, including SHIN3 cells.[35−37] The tumor model in mice was prepared as reported.[38] As a first step, we examined whether avidin-β-galactosidase could be targeted to SHIN3 cells *in vivo* by injecting it intraperitoneally into mice bearing peritoneal SHIN3 tumors. After 24 h, the organs were harvested and stained with X-Gal. After further incubation for 2 h, a blue precipitate was observed only in the disseminated tumor, confirming that avidin-β-galactosidase can be efficiently targeted to SHIN3 cells *in vivo* without loss of the enzymatic activity (Figure 5).

Fluorescence Detection of Tumors *in Vivo*. We next tried to visualize tumors prelabeled with avidin-β-galactosidase by employing **AM-TG-βGal**. In mice intraperitoneally implanted with SHIN3 and pretreated with avidin-β-galactosidase (ip), intraperitoneal administration of **AM-TG-βGal** followed by incubation for 1 h revealed strongly fluorescent spots in the peritoneal cavity (Figure 6a and 6b). Although the incubation time required for imaging is likely to vary depending on the

(33) Senter, P. D.; Saulnier, M. G.; Schreiber, G. J.; Hirschberg, D. L.; Brown, J. P.; Hellström, I.; Hellström, K. E. *Proc. Natl. Acad. Sci. U.S.A.* **1988**, *85*, 4842−4846.
(34) Senter, P. D.; Springer, C. J. *Adv. Drug Delivery Rev.* **2001**, *53*, 247−264.
(35) Hama, Y.; Urano, Y.; Koyama, Y.; Kamiya, M.; Bernardo, M.; Paik, R. S.; Krishna, M. C.; Choyke, P. L.; Kobayashi, H. *Neoplasia* **2006**, *8*, 607−612.
(36) Yao, Z.; Zhang, M.; Sakahara, H.; Saga, T.; Arano, Y.; Konishi, J. *J. Natl. Cancer. Inst.* **1998**, *90*, 25−29.
(37) Mamede, M.; Saga, T.; Kobayashi, H.; Ishimori, T.; Higashi, T.; Sato, N.; Brechbiel, M. W.; Konishi, J. *Clin. Cancer Res.* **2003**, *9*, 3756−3762.
(38) Sato, N.; Kobayashi, H.; Saga, T.; Nakamoto, Y.; Ishimori, T.; Togashi, K.; Fujibayashi, Y.; Konishi, J.; Brechbiel, M. W. *Clin. Cancer Res.* **2001**, *7*, 3606−3612.

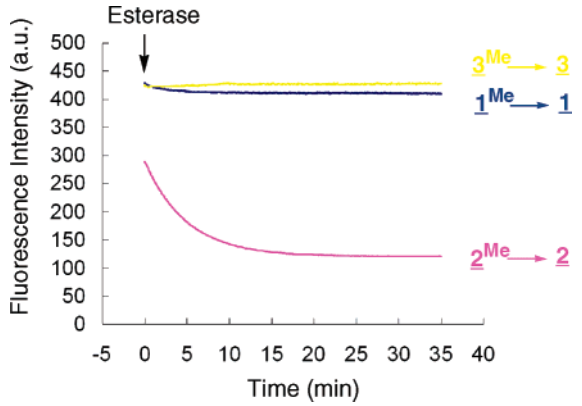

Figure 2. Fluorescence change of **1**^{Me}, **2**^{Me}, and **3**^{Me} upon reaction with esterase. Porcine liver esterase (10 units) was added at 0 min to solutions of **1**^{Me}, **2**^{Me}, and **3**^{Me} in 100 mM sodium phosphate buffer, pH 7.4, containing 0.1% DMSO as a cosolvent. Excitation and emission wavelengths were 491 and 510 nm, respectively.

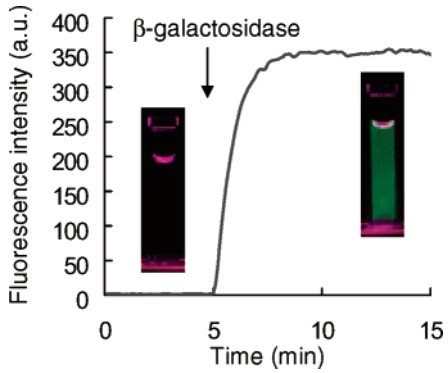

Figure 3. *In vitro* reaction of **AM-TG-*β*Gal** with *β*-galactosidase. The fluorescence increase of 1 *μ*M **AM-TG-*β*Gal** in 100 mM sodium phosphate buffer, pH 7.4, containing 1 mM $MgCl_2$, 14.3 mM 2-mercaptoethanol, 0.1% DMSO, and 6 U of *β*-galactosidase at 37 °C is shown. Excitation and emission wavelengths were 492 and 509 nm, respectively.

Table 3. Fluorescence Quantum Yields of Anionic and Neutral Forms of **1**^{Me}, **2**^{Me}, and **3**^{Me}

compound	Φ_{fl} (pH 9.0)[a]	Φ_{fl} (pH 3.4)[b]
1^{Me}	0.85	0.13
2^{Me}	0.67	0.008
3^{Me}	0.85	0.005

[a] Data for the anionic form were measured in 100 mM sodium phosphate buffer, pH 9.0, containing 0.1% DMSO as a cosolvent. [b] Data for the neutral form were measured in 100 mM sodium phosphate buffer, pH 3.4, containing 0.1% DMSO as a cosolvent. For determination of the fluorescence quantum yield, fluorescein in 100 mM aq. NaOH (0.85) was used as a fluorescence standard.[39]

size of the tumor, 1-h incubation produced clearer fluorescence signals than the 30-min incubation in our experiment. Small tumors on the mesenterium were clearly seen (Figure 6c), and fluorescence microscopy revealed spots as small as 200 *μ*m (Figure 6d). The fluorescence enhancement at microfoci over the surrounding tissues on the mesenterium is up to 33-fold (Supporting Information Figure S1). In contrast, almost no fluorescence activation could be observed in a normal, tumor-free mouse treated with avidin-*β*-galactosidase and **AM-TG-*β*Gal** (Supporting Information Figure S2). Mice given TG-*β*Gal also showed a marked fluorescence increase in the peritoneal cavity, but this was unlikely to have been confined to tumors, owing to the leakage of the fluorescent product derived from TG-*β*Gal (Figure 6e). Indeed, the fluorescence signal produced by **AM-TG-*β*Gal** at the tumors was not decreased by washing, in contrast to the case with TG-*β*Gal, suggesting that our strategy of using the hydrolyzable AM moiety did indeed improve cellular retention of the fluorescent product (Figure 7). Staining of tissue with X-Gal showed a similar distribution to that of the fluorescence signal produced by **AM-TG-*β*Gal**, indicating that the fluorescence signal was colocalized with the *β*-galactosidase activity (Figure 8). As regards the specificity of the staining, it has previously been shown that at least 99% of the small spots in the peritoneal cavity in this tumor model are tumors (Supporting Information Figure S3).[35] These results suggest that **AM-TG-*β*Gal** had been hydrolyzed both by the SHIN3-targeted *β*-galactosidase, leading to fluorescence activation, and by intraplasmic esterase, resulting in good retention within cells.

Conclusion

There is increasing interest in *in vivo* optical imaging of *β*-galactosidase in the biological and clinical fields but with limited success so far.[23−25] We have developed **AM-TG-*β*Gal** as a highly sensitive fluorescence probe for *β*-galactosidase that is suitable for targeted tumor imaging *in vivo*. It represents a development of our previously reported fluorescence probe for *β*-galactosidase,[26] modified by introducing AM ester into TG-*β*Gal through a precisely optimized linker while retaining the advantageous optical properties of TG-*β*Gal. **AM-TG-*β*Gal** exhibits a drastic fluorescence enhancement upon reaction with *β*-galactosidase and is well retained intracellularly after hydrolysis by ubiquitous intracellular esterases without loss of fluorescence. Moreover, we devised a two-step strategy for highly activatable optical imaging of intraperitoneal tumor cells without the need for prior transfection of reporter enzymes. First, a conjugate of a tumor-targeting molecule and the enzyme, avidin-*β*-galacotosidase, is administered and binds via avidin to the tumor cell surface. Second, **AM-TG-*β*Gal** is administered and is hydrolyzed to **AM-TG** by *β*-galactosidase bound to the tumor cells. **AM-TG** exhibits both highly activated fluorescence and enhanced permeability and is readily transferred into nearby tumor cells, where it is hydrolyzed to the free carboxylate by cytoplasmic esterases. This procedure provides a tumor-specific, long-lived, and highly activated fluorescence signal. Studies to examine the feasibility of using this approach in video-assisted laparoscopic surgery are in progress. The present results indicate that chemistry-based fine-tuning of chemical properties (both fluorescence and cell permeability) could be the key to the development of small-molecular "magic bullets" in the fields of biology and clinical medicine, and we believe that the range of potential applications of our new probe is enormous.

Experimental Section

All procedures were carried out in compliance with the Guide for the Care and Use of Laboratory Animal Resources (1996), National Research Council, and approved by the National Cancer Institute Animal Care and Use Committee. All experiments were carried out at 25 °C, unless otherwise specified.

Materials and Instruments. Chemicals used for organic synthesis were of the best grade available, supplied by Tokyo Chemical Industries, Wako Pure Chemical or Aldrich Chemical Co., and were used without further purification. ^{1}H NMR and ^{13}C NMR spectra were recorded on a JNM-LA300 (JEOL) instrument at 300 and 75 MHz and on a JNM-

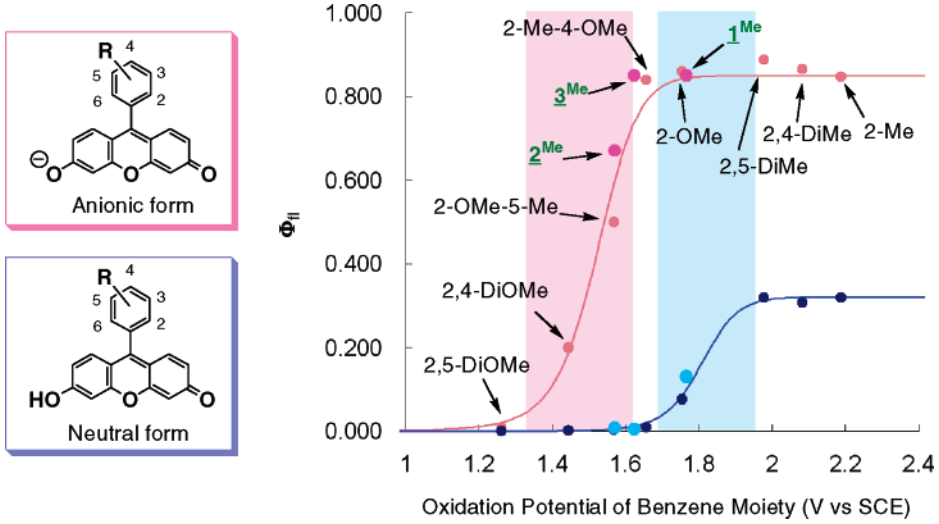

Figure 4. Relationship between the oxidation potential of the benzene moiety and Φ_{fl} of the anion form (red) and neutral form (blue). Data for previously reported TokyoGreen derivatives[26] and the newly developed **1**^{Me}, **2**^{Me}, and **3**^{Me} are depicted on the same graph. The curve represents the best fit to the Marcus equation.

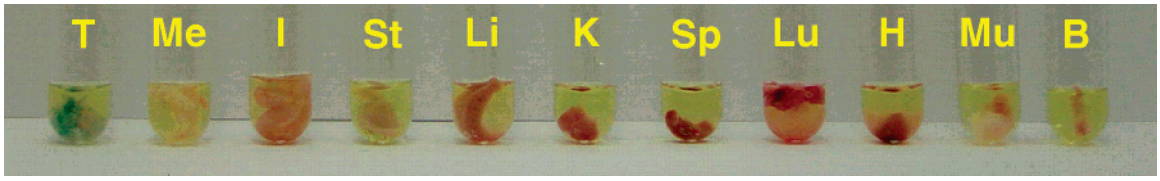

Figure 5. *In vivo* targeting of avidin-β-galactosidase to intraperitoneal SHIN3 tumors in mouse. Avidin-β-galactosidase (100 μg) in PBS(-) was injected intraperitoneally into a SHIN3-implanted mouse, and after 20 h the mouse was sacrificed. The main internal organs (tumor (T), mesentery (Me), intestine (I), stomach (St), liver (Li), kidney (K), spleen (Sp), lung (Lu), heart (H), muscle (Mu), bone (B)) were removed and stained with X-Gal for 2 h.

AL400 (JEOL) instrument at 400 MHz. Mass spectra (MS) were measured with an SX-102A (JEOL) for EI, an MS700 (JEOL) for FAB, and a JMS-T100LC (JEOL) for ESI-TOF.

UV/vis and Fluorescence Analysis. For the absorption or fluorescence measurement, compounds were dissolved in dimethyl sulfoxide (DMSO, fluorometric grade, Dojindo) to obtain 10 mM stock solutions. These stock solutions were diluted with buffer as specified in the figure legends to the desired concentration. For determination of the quantum efficiency of fluorescence (Φ_{fl}), fluorescein in 100 mM aq. NaOH (Φ_{fl} = 0.85) was used as a fluorescence standard.[39] β-Galactosidase and porcine liver esterase were purchased from Sigma-Aldrich Japan K.K. All absorption spectra were obtained with a 8453 UV/vis spectrometer (Agilent) or with a UV-1600 UV/vis spectrometer (Shimadzu). All fluorescence spectra were obtained with an LS-55 fluorescence spectrometer (Perkin-Elmer) or an F4500 fluorescence spectrometer (Hitachi).

Cyclic Voltammetry. Cyclic voltammetry was performed on a 600A electrochemical analyzer (ALS). A three-electrode arrangement in a single cell was used for the measurements: a Pt wire as the auxiliary electrode, a glassy carbon electrode as the working electrode, and a Ag/Ag^+ electrode as the reference electrode. The sample solutions contained a 1.0 mM sample and 100 mM tetrabutylammonium perchlorate (TBAP) as a supporting electrolyte in acetonitrile, and argon was bubbled for 10 min before each measurement. Obtained potentials (vs Ag/Ag^+) were converted to those vs SCE by adding 0.248 V.

Photochemical Calculation. HOMO energy levels were calculated at the B3LYP/6-31G level with Gaussian 98W.

Intracellular Retention Assay. HEK293 cells expressing β-galactosidase were incubated with a 10 μM solution of TG-βGal or AM-TG-βGal in physiological salt solution, pH 7.4, containing 150 mM NaCl, 4 mM KCl, 2 mM $CaCl_2$, 1 mM $MgCl_2$, 5 mM HEPES, and 0.1% glucose (PSS), and 0.1% DMSO as a cosolvent for 2 h. Then, confocal fluorescence images and DIC images were captured before and after washing with PSS. The images were obtained with an Olympus fluoview system using an IX81 inverted microscope, an Ar ion laser, and a PlanApo 40x/1.40 objective lens (Olympus, Tokyo, Japan). The excitation wavelength was 488 nm, and the emission wavelength was 510−550 nm.

Mouse Preparation. The intraperitoneal tumor model was prepared as previously reported.[38] Briefly, 2×10^6 SHIN3 cancer cells suspended in PBS(-) were injected intraperitoneally into female nude mice (National Cancer Institute Animal Production Facility, Frederick, MD). Experiments with these tumor-harboring mice were performed at 10−13 days after dissemination, when numerous small, intraperitoneally disseminated tumors had formed, especially around the stomach, the subphrenic region, at the hepatic and splenic hila, and on the mesentery.

Biodistribution of Avidin-β-galactosidase *in Vivo*. Avidin-β-galactosidase (100 μg) in PBS(-) was injected intraperitoneally into tumor-bearing mice. After 20 h, the mice were sacrificed by exposure to CO_2 gas. The main internal organs (tumor, mesentery, intestine, stomach, liver, kidney, spleen, lung, heart) were removed for routine X-Gal staining.

Fluorescence Imaging of Tumors in a Mouse Tumor Model. Avidin-β-galactosidase (100 μg) in PBS(-) was injected intraperitoneally into a tumor-bearing mouse, which was left for 16−23 h. Then, a 3.3 μM solution of AM-TG-βGal was injected. After 1 h, the mouse was sacrificed under anesthesia, and the abdominal walls were removed. Fluorescence images in the peritoneal cavity were captured with a Maestro In-Vivo Imaging System (CRI Inc., Woburn, MA). The excitation wavelength was 445−490 nm. Spectral unmixing was performed to obtain the fluorescence unmixed images. Fluorescence images of tumor nodules on the mesentery were captured with a BX51

(39) Paeker, C. A.; Rees, W. T. *Analyst* **1960**, *85*, 587−600.

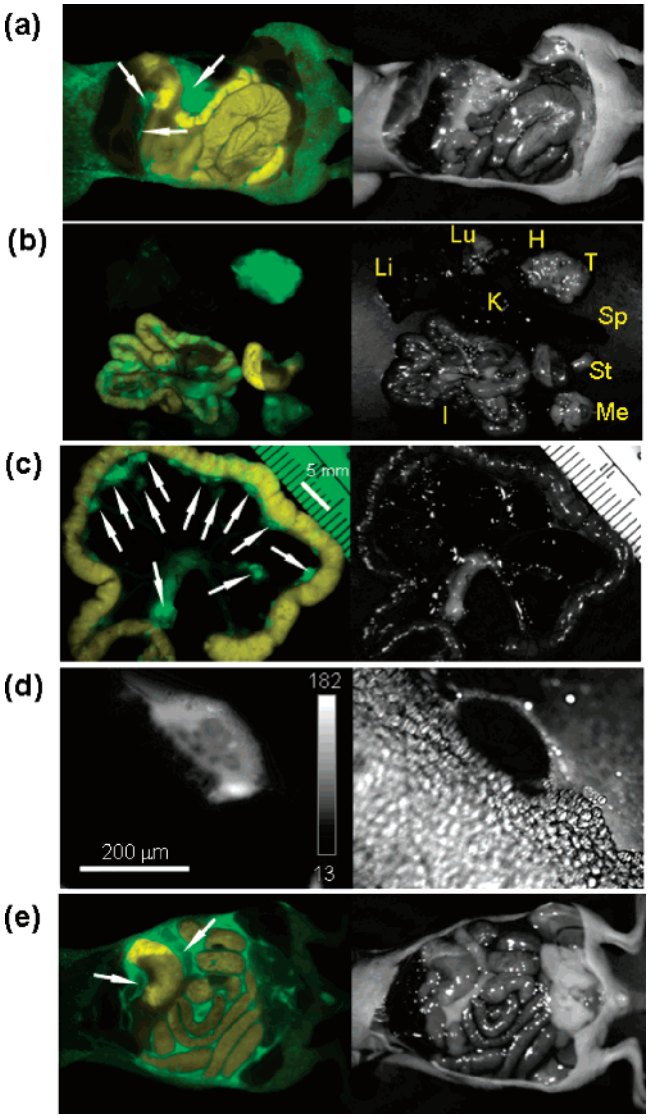

Figure 6. *Ex vivo* fluorescence imaging of SHIN3-targeted β-galactosidase activity with **AM-TG-βGal** or TG-βGal. (a) Tumors were imaged with **AM-TG-βGal**, following pretreatment with avidin-β-galactosidase. Tumors (arrows) were clearly visualized with a high tumor-to-nontumor signal ratio. (b) *Ex vivo* fluorescence imaging of the main internal organs of the mouse. T, tumor; Me, mesentery; I, intestine; St, stomach; Li, liver; K, kidney; Sp, spleen; Lu, lung; H, heart. (c) Magnified image of a peritoneal tumor. Strong fluorescence signals reveal tiny peritoneal tumor nodules (arrows). (d) Fluorescent microfoci as small as 200 μm in diameter can be seen by using fluorescence microscopy. (e) Tumor imaging with TG-βGal, following pretreatment with avidin-β-galactosidase. Strong fluorescence was observed in the peritoneal cavity; however, this was unlikely to have been confined to tumors, owing to the rapid leakage of its fluorescent product. The unmixed fluorescence images (left) and white light images (right) of (a), (b), (c), and (e) were captured with a Maestro In-Vivo Imaging System (CRI Inc., Woburn, MA). To obtain the unmixed fluorescence images, spectral division was performed using the autofluorescence of intestine (yellow) and the fluorescence at the tumor (green). The fluorescence image (left) and DIC image (right) of (d) were captured with a BX51 microscope (Olympus USA, Melville, NY).

microscope (Olympus USA, Melville, NY) equipped with an UPLAPO10x objective lens (Olympus USA, Melville, NY).

Synthesis of 2-Bromo-5-(*tert*-butyldimethylsilyloxy)toluene (1). A mixture of 4-bromo-3-methylphenol (2 g, 10.7 mmol), *tert*-butyldimethylsilyl chloride (TBDMS−Cl) (4.8 g, 30 mmol), and imidazole (3.6 g, 50 mmol) in dry DMF (10 mL) was stirred at room temperature under argon for 3 h. The solvent was concentrated under reduced pressure. The residue was diluted with water and extracted with CH_2Cl_2 three times. The combined organic solution was washed with water and saturated aq. NaCl, dried over Na_2SO_4, and evaporated to give **1** as a colorless clear oil (3.04 g, 95%). ^{1}H NMR (300 MHz, $CDCl_3$) δ 7.33 (d, 1H, J = 8.6 Hz), 6.72 (d, 1H, J = 2.9 Hz), 6.53 (dd, 1H, J = 8.6 Hz, 2.9 Hz), 2.32 (s, 3H), 0.97 (s, 9H), 0.18 (s, 6H); ^{13}C NMR (75 MHz, $CDCl_3$) δ 154.88, 138.79, 132.76, 122.59, 119.10, 116.16, 25.64, 22.98, 18.18, −4.48. MS (FAB): m/z 301, 303 $[M + H]^+$.

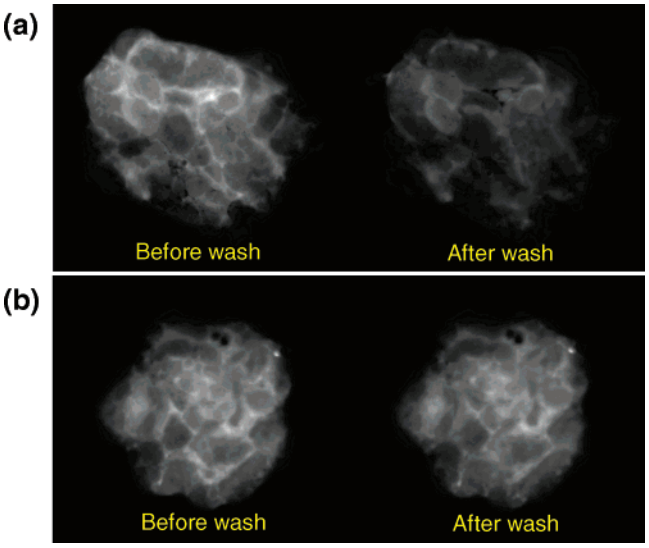

Figure 7. Fluorescence images of SHIN3 tumors removed from a mouse after incubation with TG-βGal (a) or **AM-TG-βGal** (b), before and after washing with PBS.

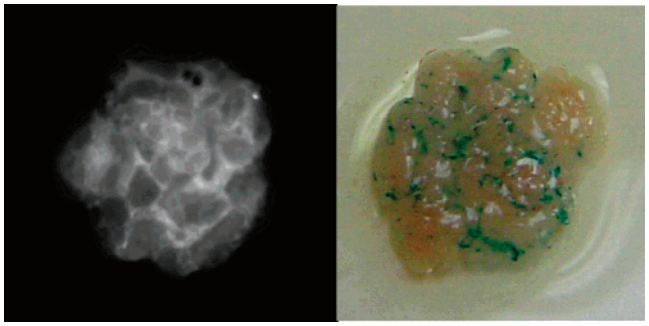

Figure 8. Distribution of β-galactosidase activity in the removed tumor. Avidin-β-galactosidase was intraperitoneally injected into SHIN3-implanted mouse, and then **AM-TG-βGal** was administered. The tumor was removed and stained with X-Gal for 1 h.

Synthesis of 9-{1-[4-(*tert*-Butyldimethylsilyloxy)-2-methylphenyl]}-6-hydroxy-3*H*-xanthen-3-one (2). A solution of **1** (1.28 g, 4.27 mmol) in distilled THF (10 mL) was cooled down to −78 °C (dry ice−acetone). *tert*-Butyllithium in an *n*-pentane solution (4.5 mL, 6.57 mmol) was added dropwise to the reaction mixture using a syringe. 3,6-Bis-(*tert*-butyldimethylsilanyloxy)xanthen-9-one (1.07 g, 2.37 mmol) dissolved in distilled THF (20 mL) was added dropwise to the mixture using a syringe. The mixture was stirred at −78 °C under argon for 30 min, then 2 N aq. HCl was added, and the red precipitate was collected by filtration. The precipitate was chromatographed on silica gel with CH_2Cl_2−MeOH (100:3−100:5) as the eluent to give **2** as an orange powder (774.6 mg, 82%). ^{1}H NMR (300 MHz, CD_3OD) δ 7.27 (d, 2H, J = 9.2 Hz), 7.15 (d, 1H, J = 8.3 Hz), 7.01−6.86 (m, 6H), 2.01 (s, 3H), 1.06 (s, 9H), 0.31 (s, 6H). HRMS(ESI$^-$): calcd for $[M - H]^-$, 431.167 86; found, 431.166 36.

Synthesis of 9-[1-(4-Hydroxy-2-methylphenyl)]-6-hydroxy-3*H*-xanthen-3-one (3). To a solution of **2** (2.62 g, 6.2 mmol) in distilled THF (200 mL) a 1 M solution of tetrabutylammonium fluoride in THF (6.2 mL, 6.2 mmol) was added. The mixture was stirred at room

temperature under argon for 2 h and then evaporated, and the residue was chromatographed on silica gel with CH_2Cl_2−MeOH (100:5−100:7) as the eluent to give **3** as an orange powder (1.13 g, 58%). ^{1}H NMR (300 MHz, CD_3OD) δ 7.06 (d, 2H, J = 9.7 Hz), 6.94 (d, 1H, J = 8.2 Hz), 6.78 (d, 1H, J = 2.4 Hz), 6.74 (dd, 1H, J = 8.2 Hz, 2.4 Hz), 6.63 (dd, 2H, J = 9.7 Hz, 2.0 Hz), 6.63 (d, 2H, J = 2.0 Hz), 1.88 (s, 3H); ^{13}C NMR (75 MHz, $CDCl_3$) δ 172.60, 168.75, 161.03, 160.78, 138.82, 134.65, 131.78, 122.84, 121.30, 118.66, 118.29, 114.30, 103.40, 20.25. HRMS (ESI^+): calcd for $[M + H]^+$, 319.09703; found, 319.09652.

Synthesis of 9-[1-(4-Methoxycarbonylmethoxy-2-methylphenyl)]-6-hydroxy-3*H*-xanthen-3-one (4). To a mixture of **3** (60 mg, 0.18 mmol) and Cs_2CO_3 (400 mg, 1.2 mmol) in dry dimethylformamide (5 mL), methyl bromoacetate (17 μL, 0.18 mmol) was added. The reaction mixture was stirred at room temperature under argon overnight. The inorganic precipitate was filtered off, and the filtrate was concentrated under reduced pressure. The residue was diluted with water and extracted with CH_2Cl_2 three times. The combined organic solution was washed with water and saturated aq. NaCl, dried over Na_2SO_4, and evaporated. The residue was chromatographed on silica gel with CH_2Cl_2−MeOH (100:5) as the eluent to give **4** as a red powder (41.7 mg, 57%). ^{1}H NMR (300 MHz, $CDCl_3$) δ 7.10 (d, 1H, J = 8.4 Hz), 7.08 (d, 2H, J = 9.2 Hz), 6.95 (d, 1H, J = 2.5 Hz), 6.89 (dd, 1H, J = 8.4 Hz, 2.5 Hz), 6.84 (d, 2H, J = 2.0 Hz), 6.80 (dd, 2H, J = 9.2 Hz, 2.0 Hz), 4.73 (s, 2H), 3.86 (s, 3H), 2.03 (s, 3H). HRMS (ESI^+): calcd for $[M + H]^+$, 391.118 16; found, 391.114 55.

Synthesis of 9-[1-(4-Methoxycarbonylmethoxy-2-methylphenyl)]-6-hydroxy-3*H*-xanthen-3-one Mono(2′,3′,4′,6′-tetra-*O*-acetyl-β-D-galactopyranoside) (5). A mixture of **4** (39 mg, 0.1 mmol), Cs_2CO_3 (200 mg, 0.6 mmol), and 2,3,4,6-tetra-*O*-acetyl-α-D-galactopyranosyl bromide (100 mg, 0.25 mmol) in dry dimethylformamide (2 mL) was stirred at room temperature under argon overnight. The inorganic precipitate was filtered off, and the filtrate was concentrated under reduced pressure. The residue was diluted with water and extracted with CH_2Cl_2 three times. The combined organic solution was washed with water and saturated aq. NaCl, dried over Na_2SO_4, and evaporated. The residue was chromatographed on silica gel with CH_2Cl_2−MeOH (100:3) as the eluent to give **5** as an orange powder (41.8 mg, 58%). ^{1}H NMR (300 MHz, $CDCl_3$) δ 7.10−6.80 (m, 7H), 6.57 (dd, 1H, J = 9.7 Hz, 1.9 Hz), 6.40 (d, 1H, J = 1.9 Hz), 5.57−5.48 (m, 2H), 5.18−5.12 (m, 2H), 4.73 (s, 2H), 4.22−4.16 (m, 3H), 3.87 (s, 3H), 2.19 (s, 3H), 2.13 (s, 3H), 2.07 (s, 3H), 2.03 (s, 3H), 2.05 (s, 3H). HRMS (ESI^+): calcd for $[M + Na]^+$, 743.19519; found, 743.19309.

Synthesis of 9-[1-(4-Methoxycarbonylmethoxy-2-methylphenyl)]-6-hydroxy-3*H*-xanthen-3-one Mono-β-D-galactopyranoside (6). To a solution of **5** (5 mg, 6.9 μmol) in methanol (2 mL) a 5 M methanol solution of NaOMe (2 μL, 10 μmol) was added. The mixture was stirred at room temperature for 1 h and then neutralized with Amberlite IR-120 (H^+). The Amberlite IR-120 was filtered off, and the filtrate was evaporated. The residue was chromatographed on silica gel with $CHCl_3$−MeOH (100:10) as the eluent to give **6** as an orange powder (2.4 mg, 62%). ^{1}H NMR (300 MHz, CD_3OD) δ 7.36 (d, 1H, J = 2.2 Hz), 7.18 (d, 1H, J = 9.0 Hz), 7.17 (d, 1H, J = 8.4 Hz), 7.15 (d, 1H, J = 9.6 Hz), 7.07−7.12 (m, 1H), 7.06 (d, 1H, J = 2.6 Hz), 7.00 (dd, 1H, J = 8.4, 2.6 Hz), 6.61 (dd, 1H, J = 9.6, 2.0 Hz), 6.47 (d, 1H, J = 2.0 Hz), 5.10 (dd, 1H, J = 7.7, 2.6 Hz), 4.84 (s, 2H), 3.92 (d, 1H, J = 3.5 Hz), 3.82 (s, 3H), 3.73−3.89 (m, 4H), 3.62 (dd, 1H, J = 9.7, 3.3 Hz), 2.03 (s, 3H). HRMS(ESI^+): calcd for $[M + H]^+$, 553.17099; found, 553.16771.

Synthesis of 9-[1-(4-Carboxymethoxy-2-methylphenyl)]-6-hydroxy-3*H*-xanthen-3-one (7). To a solution of **4** (15 mg, 38 μmol) in methanol (4 mL) 2 M aq. NaOH (1 mL, 2 mmol) was added. The mixture was stirred at room temperature for 4 h and then neutralized with 2 N aq. HCl. The methanol was evaporated off, and the residue was diluted with H_2O and extracted with CH_2Cl_2. The combined organic layer was evaporated, and the residue was chromatographed on silica gel with CH_2Cl_2−MeOH (100:5) as the eluent to give **7** as an orange powder (12 mg, 83%). ^{1}H NMR (300 MHz, CD_3OD) δ 7.00 (d, 1H, J = 8.4 Hz), 6.93−6.88 (m, 2H), 6.88 (d, 2H, J = 9.0 Hz), 6.44 (dd, 2H, J = 9.0, 2.1 Hz), 6.41 (d, 2H, J = 2.1 Hz), 4.39 (s, 2H), 1.92 (s, 3H). HRMS (ESI^-): calcd for $[M - H]^-$, 375.086 86; found, 375.087 79.

Synthesis of 2-Bromo-5-(toluene-4-sulfonyloxy)anisole (8). A mixture of 4-bromoresorcinol (2.0 g, 10.5 mmol), *p*-toluenesulfonyl chloride (2.21 g, 11.6 mmol), and K_2CO_3 (4.4 g, 32 mmol) in dry acetone (150 mL) was refluxed overnight. MeI (1.3 mL, 21 mmol) was added, and the reaction mixture was refluxed overnight again. The inorganic precipitate was filtered off, and the filtrate was concentrated under reduced pressure. The residue was diluted with water and extracted with AcOEt three times. The combined organic solution was washed with water and saturated aq. NaCl, dried over Na_2SO_4, and evaporated to give **8** as a light pink oil (3.8 g, quant.). ^{1}H NMR (300 MHz, $CDCl_3$) δ 7.72 (d, 2H, J = 8.3 Hz), 7.40 (d, 1H, J = 8.6 Hz), 7.33 (d, 2H, J = 8.3 Hz), 6.59 (d, 1H, J = 2.5 Hz), 6.40 (dd, 1H, J = 8.6 Hz, 2.5 Hz), 3.78 (s, 3H), 2.45 (s, 3H); ^{13}C NMR (75 MHz, $CDCl_3$) δ 156.47, 156.25, 133.04, 113.19, 105.06, 103.03, 56.08, 25.64, 18.19, −4.45. MS (EI): 356, 358 (M^+).

Synthesis of 4-Bromo-3-methoxyphenol (9). To a solution of **8** (3.08 g, 8.6 mmol) in distilled MeOH (100 mL) 2 N aq. NaOH (20 mL) was added. The solution was refluxed for 1.5 h, and then the solvent was evaporated. The obtained residue was neutralized with 2 N aq. HCl and extracted with CH_2Cl_2 three times. The organic solution was washed with water and saturated aq. NaCl, dried over Na_2SO_4, and evaporated to give **9** as a clear oil (1.57 g, 89%). ^{1}H NMR (300 MHz, $CDCl_3$) δ 7.34 (d, 1H, J = 8.6 Hz), 6.45 (d, 1H, J = 2.7 Hz), 6.32 (dd, 1H, J = 8.6 Hz, 2.7 Hz), 3.86 (s, 3H). MS (EI): 202, 204 (M^+).

Synthesis of 2-Bromo-5-(*tert*-butyldimethylsilyloxy)anisole (10). A mixture of **9** (1.57 g, 7.7 mmol), TBDMS−Cl (3.5 g, 23 mmol), and imidazole (2.6 g, 39 mmol) in dry DMF (10 mL) was stirred at room temperature under argon overnight. The solvent was concentrated under reduced pressure. The residue was diluted with water and extracted with CH_2Cl_2 three times. The combined organic solution was washed with water and saturated aq. NaCl, dried over Na_2SO_4, and evaporated. The residue was chromatographed on silica gel with hexane−AcOEt (4:1) as the eluent to give **10** as a light yellow clear oil (1.88 g, 76.7%). ^{1}H NMR (300 MHz, $CDCl_3$) δ 7.33 (d, 1H, J = 8.6 Hz), 6.41 (d, 1H, J = 2.6 Hz), 6.34 (dd, 1H, J = 8.6 Hz, 2.6 Hz), 3.85 (s, 3H), 0.98 (s, 9H), 0.20 (s, 6H); ^{13}C NMR (75 MHz, $CDCl_3$) δ 156.46, 149.55, 145.61, 133.28, 132.03, 129.80, 128.59, 115.20, 109.92, 106.97, 56.34, 21.70. MS (EI): 316, 318 (M^+).

Synthesis of 9-{1-[4-(*tert*-Butyldimethylsilyloxy)-2-methoxyphenyl]}-6-hydroxy-3*H*-xanthen-3-one (11). 10 (1.39 g, 4.4 mmol) was dissolved in distilled THF (10 mL), and the solution was cooled to −78 °C (dry ice−acetone). *tert*-Butyllithium in *n*-pentane solution (4.5 mL, 6.57 mmol) was added dropwise to the reaction mixture, and then 3,6-bis(*tert*-butyldimethylsilanyloxy)xanthen-9-one (1.19 g, 2.6 mmol) dissolved in 20 mL of distilled THF was further added dropwise. The mixture was stirred at −78 °C under argon for 30 min, and 2 N aq. HCl was added. The solvent was evaporated under reduced pressure to leave a residue, which was diluted with water and extracted with CH_2Cl_2 three times. The combined organic solution was washed with water and saturated aq. NaCl, dried over Na_2SO_4, and evaporated. The precipitate was chromatographed on silica gel with CH_2Cl_2−MeOH (100:5) as the eluent to give **11** as an orange powder (43.6 mg, 3.7%). ^{1}H NMR (300 MHz, $CDCl_3$) δ 7.18 (d, 2H, J = 9.0 Hz), 7.02 (d, 1H, J = 8.3 Hz), 6.80−6.75 (m, 4H), 6.60 (dd, 1H, J = 8.3 Hz, 2.0 Hz), 6.56 (d, 1H, J = 2.0 Hz), 3.67 (s, 3H), 1.04 (s, 9H), 0.31 (s, 6H). HRMS (ESI^+): calcd for $[M + H]^+$, 449.178 42; found, 449.177 90.

Synthesis of 9-[1-(4-Hydroxy-2-methoxyphenyl)]-6-hydroxy-3*H*-xanthen-3-one (12). To a solution of **11** (43.6 mg, 97 μmol), 2 N aq. HCl (2 mL) was added, and the mixture was refluxed for 5 h. The solvent was evaporated under reduced pressure. The obtained residue was chromatographed on silica gel with CH_2Cl_2−MeOH (100:5) as

the eluent to give **12** as a red powder (22.7 mg, 70%). ^{1}H NMR (300 MHz, CD_3OD): δ 7.82 (d, 2H, J = 9.2 Hz), 7.32 (d, 2H, J = 2.4 Hz), 7.24 (dd, 2H, J = 9.2 Hz, 2.4 Hz), 7.18 (d, 1H, J = 8.3 Hz), 6.76 (d, 1H, J = 2.0 Hz), 6.70 (dd, 1H, J = 8.3 Hz, 2.0 Hz), 3.70 (s, 3H). HRMS (ESI$^+$): calcd for $[M + H]^+$, 335.091 95; found, 335.088 62.

Synthesis of 9-[1-(2-Methoxy-4-methoxycarbonylmethoxyphenyl)]-6-hydroxy-3*H*-xanthen-3-one (13). A mixture of **12** (22.7 mg, 68 μmol), bromomethyl acetate (6.27 μL, 68 μmol), and Cs_2CO_3 (66.5 mg, 204 μmol) was stirred at room temperature under argon overnight. The inorganic precipitate was filtered off, and the filtrate was concentrated under reduced pressure. The residue was diluted with water and extracted with CH_2Cl_2 three times. The combined organic solution was washed with water and saturated aq. NaCl, dried over Na_2SO_4, and evaporated. The residue was chromatographed on silica gel with CH_2Cl_2−MeOH (100:5) as the eluent to give **13** as an orange powder (17.4 mg, 63%). ^{1}H NMR (300 MHz, $CDCl_3$) δ 7.16 (d, 2H, J = 9.0 Hz), 7.10 (d, 1H, J = 8.3 Hz), 6.81 (m, 3H), 6.75 (dd, 2H, J = 9.0 Hz, 2.0 Hz), 6.59 (dd, 1H, J = 8.3 Hz, 2.2 Hz,), 4.74 (s, 2H), 3.87 (s, 3H), 3.69 (s, 3H). HRMS (ESI$^+$): calcd for $[M + H]^+$, 407.113 08; found, 407.110 06.

Synthesis of 9-[1-(2-Methoxy-4-methoxycarbonylmethoxyphenyl)]-6-hydroxy-3*H*-xanthen-3-one Mono(2′,3′,4′,6′-tetra-*O*-acetyl-β-D-galactopyranoside) (14). A mixture of **13** (3.8 mg, 9.3 μmol), Cs_2CO_3 (38.4 mg, 117 μmol), and 2,3,4,6-tetra-*O*-acetyl-α-D-galactopyranosyl bromide (100 mg, 0.25 mmol) in dry DMF (2 mL) was stirred at room temperature under argon for 4.5 h. The inorganic precipitate was filtered off, and the filtrate was concentrated under reduced pressure. The residue was diluted with water and extracted with CH_2Cl_2 three times. The combined organic solution was washed with water and saturated aq. NaCl, dried over Na_2SO_4, and evaporated. The residue was chromatographed on silica gel with CH_2Cl_2−MeOH (100:3) as the eluent to give **14** as an orange powder (6.4 mg, 94.2%). ^{1}H NMR (300 MHz, $CDCl_3$) δ 7.13−7.06 (m, 4H), 6.81 (dd, 1H, J = 8.8 Hz, 2.4 Hz), 6.74 (d, 1H, J = 2.3 Hz), 6.59 (dd, 1H, J = 8.2 Hz, 2.3 Hz), 6.57 (dd, 1H, J = 9.7 Hz, 1.8 Hz), 6.39 (d, 1H, J = 1.8 Hz), 5.56−5.49 (m, 2H), 5.18−5.13 (m, 2H), 4.74 (s, 2H), 4.25−4.17 (m, 3H), 3.86 (s, 3H), 3.70 (s, 3H), 2.20 (s, 3H), 2.14 (s, 3H), 2.07 (s, 3H), 2.03(s, 3H). HRMS (ESI$^+$): calcd for $[M + H]^+$, 737.208 16; found, 737.208 60.

Synthesis of 9-[1-(2-Methoxy-4-methoxycarbonylmethoxyphenyl)]-6-hydroxy-3*H*-xanthen-3-one Mono-β-D-galactopyranoside) (15). To a solution of **14** (2 mg, 2.7 μmol) in methanol (1 mL) a 5 M methanol solution of NaOMe (2 μL, 5 μmol) was added. The mixture was stirred at room temperature for 1 h and then neutralized with Amberlite IR-120 (H^+). The Amberlite IR-120 was filtered off, and the filtrate was evaporated. The residue was chromatographed on silica gel with $CHCl_3$−MeOH (100:10) as the eluent to give **15** as an orange powder (0.74 mg, 48%). ^{1}H NMR (400 MHz, CD_3OD): δ 7.35 (d, 1H, J = 2.4 Hz), 7.30 (d, 1H, J = 9.3 Hz), 7.27 (d, 1H, J = 9.8 Hz), 7.19 (d, 1H, J = 8.3 Hz), 7.11 (dd, 1H, J = 9.3, 2.4 Hz), 6.88 (d, 1H, J = 2.2 Hz), 6.77 (dd, 1H, J = 8.3, 2.2 Hz), 6.62 (dd, 1H, J = 9.8, 2.0 Hz), 6.46 (d, 1H, J = 2.0 Hz), 5.10 (dd, 1H, J = 7.3, 1.5 Hz), 4.78 (s, 2H), 3.93 (d, 1H, J = 2.4 Hz), 3.89−3.75 (m, 4H), 3.73 (s, 3H), 3.70−3.69 (m, 1H), 3.65 (s, 3H). HRMS (ESI$^+$): calcd for $[M + H]^+$, 569.165 90; found, 569.168 46.

Synthesis of 9-[1-(4-Carboxymethoxy-2-methoxyphenyl)]-6-hydroxy-3*H*-xanthen-3-one (16). To a solution of **13** (4.1 mg, 10 μmol) in methanol (1 mL) 2 N aq. NaOH (0.1 mL, 0.2 mmol) was added. The mixture was stirred at room temperature for 4 h and then neutralized with 2 N aq. HCl. The solvent was evaporated off, and the residue was subjected to reversed-phase preparative TLC (RP18W) with acetonitrile/water (1:1) as the eluent to give **16** as an orange powder (3 mg, 76%). ^{1}H NMR (300 MHz, CD_3OD) δ 7.25 (d, 2H, J = 9.17 Hz), 7.12 (d, 1H, J = 8.25 Hz), 6.84 (d, 1H, J = 2.20 Hz), 6.74 (dd, 1H, J = 8.25, 2.20 Hz), 6.66−6.72 (m, 4H), 4.52 (s, 2H), 3.73 (s, 3H). HRMS (ESI$^-$): calcd for $[M - H]^-$, 391.081 78; found, 391.079 47.

Synthesis of 9-{1-[4-(4-Methoxycarbonylbutyloxy)-2-methylphenyl]}-6-hydroxy-3*H*-xanthen-3-one (17). To a mixture of **3** (63.8 mg, 0.20 mmol) and Cs_2CO_3 (400 mg, 1.2 mmol) in dry dimethylformamide (2 mL) methyl 5-bromovalerate (21 μL, 0.18 mmol) was added. The reaction mixture was stirred at room temperature under argon overnight. The inorganic precipitate was filtered off, and the filtrate was concentrated under reduced pressure. The residue was diluted with water and extracted with CH_2Cl_2 three times. The combined organic solution was washed with water and saturated aq. NaCl, dried over Na_2SO_4, and evaporated. The residue was chromatographed on silica gel with CH_2Cl_2−MeOH (100:5) as the eluent to give **17** as a red powder (53.7 mg, 62%). ^{1}H NMR (300 MHz, $CDCl_3$) δ 7.10 (d, 2H, J = 9.2 Hz), 7.07 (d, 1H, J = 8.3 Hz), 6.91−6.84 (m, 4H), 6.81 (dd, 2H, J = 9.2 Hz, 2.0 Hz), 4.06 (m, 2H), 3.70 (s, 3H), 2.45 (m, 2H), 2.02 (s, 3H), 1.88 (m, 4H); ^{13}C NMR (75 MHz, $CDCl_3$) δ 175.04, 174.08, 159.73, 157.43, 152.90, 137.67, 130.77, 130.21, 124.47, 121.80, 116.42, 115.57, 111.84, 103.68, 67.41, 53.35, 33.58, 28.54, 21.55, 19.83. HRMS (ESI$^+$): calcd for $[M + H]^+$, 433.165 11; found, 433.168 53.

Synthesis of 9-{1-[4-(4-methoxycarbonylbutyloxy)-2-methylphenyl]}-6-hydroxy-3*H*-xanthen-3-one Mono(2′,3′,4′,6′-tetra-*O*-acetyl-β-D-galactopyranoside) (18). A mixture of **17** (18.2 mg, 42 μmol), Cs_2CO_3 (250 mg, 0.77 mmol), and 2,3,4,6-tetra-*O*-acetyl-α-D-galactopyranosyl bromide (100 mg, 0.25 mmol) in dry dimethylformamide (1 mL) was stirred at room temperature under argon overnight. The inorganic precipitate was filtered off, and the filtrate was concentrated under reduced pressure. The residue was diluted with water and extracted with CH_2Cl_2 three times. The combined organic solution was washed with water and saturated aq. NaCl, dried over Na_2SO_4, and evaporated. The residue was chromatographed on silica gel with AcOEt as the eluent to give **18** as an orange powder (25 mg, 78%). ^{1}H NMR (300 MHz, $CDCl_3$) δ 7.08−6.80 (m, 7H), 6.57 (dd, 1H, J = 9.7 Hz, 2.0 Hz), 6.39 (d, 1H, J = 2.0 Hz), 5.56−5.48 (m, 2H), 5,18−5.12 (m, 2H), 4.22−4.11 (m, 3H), 4.06 (m, 2H), 3.70 (s, 3H), 2.19 (s, 3H), 2.13 (s, 3H), 2.07 (s, 3H), 2.03 (s, 3H), 1.88 (m, 4H). HRMS (ESI$^+$): calcd for $[M + H]^+$, 763.260 19; found, 763.255 43.

Synthesis of 9-{1-[4-(4-methoxycarbonylbutyloxy)-2-methylphenyl]}-6-hydroxy-3*H*-xanthen-3-one Mono-β-D-galactopyranoside (19). To a solution of **18** (28 mg, 37 μmol) in methanol (5 mL) a 5 M methanol solution of NaOMe (10 μL, 50 μmol) was added. The mixture was stirred at room temperature for 1 h and then neutralized with Amberlite IR-120 (H^+). The Amberlite IR-120 was filtered off, and the filtrate was evaporated. The residue was subjected to reversed-phase preparative TLC (RP18W) with acetonitrile/water (1:1) as the eluent to give **19** as an orange powder (7.4 mg, 34%). ^{1}H NMR (300 MHz, CD_3OD) δ 7.37 (d, 1H, J = 2.4 Hz), 7.19 (dd, 1H, J = 8.8 Hz), 7.16 (d, 1H, J = 9.7 Hz), 7.15 (d, 1H, J = 8.3 Hz), 7.10 (d, 1H, J = 8.3 Hz, 2.4 Hz), 7.03 (d, 1H, J = 1.8 Hz), 6.99 (dd, 1H, J = 8.3 Hz, 1.8 Hz), 6.61 (dd, 1H, J = 9.7 Hz, 2.0 Hz), 6.47 (d, 1H, J = 2.0 Hz), 4.10 (m, 2H), 5.10 (dd, 1H, J = 7.7 Hz, 3.0 Hz), 3.92 (d, 1H, J = 3.5 Hz), 3.88−3.74 (m, 4H), 3.62 (dd, 1H, J = 9.5 Hz, 3.1 Hz), 3.67 (s, 3H), 2.45 (m, 2H), 2.06 (s, 3H), 1.88 (m, 4H). HRMS (ESI$^+$): calcd for $[M + H]^+$, 595.217 94; found, 595.218 62.

Synthesis of 9-{1-[4-(4-Carboxybutyloxy)-2-methylphenyl]}-6-hydroxy-3*H*-xanthen-3-one (20). To a solution of **17** (9.3 mg, 21.5 μmol) in methanol (2 mL) 2 M aq. NaOH (0.5 mL, 1 mmol) was added. The mixture was stirred at room temperature for 4 h and then neutralized with 2 N aq. HCl. The methanol was evaporated off, and the residue was diluted with H_2O and then extracted with CH_2Cl_2. The combined organic layer was evaporated, and the residue was chromatographed on silica gel with CH_2Cl_2−MeOH (100:5) as the eluent to give **20** as an orange powder (7 mg, 78%). ^{1}H NMR (300 MHz, CD_3OD) δ 7.11−7.16 (m, 3H), 7.03 (d, 1H, J = 2.6 Hz), 6.98 (dd, 1H, J = 8.4, 2.6 Hz), 6.70−6.75 (m, 4H), 4.10 (t, 2H, J = 5.6 Hz), 2.40 (t, 2H, J = 6.8 Hz),

2.02 (s, 3H), 1.92−1.78 (m, 4H). HRMS (ESI$^-$): calcd for [M − H]$^-$, 417.133 81; found, 417.130 84.

Synthesis of 9-{1-[4-(4-Carboxybutyloxy)-2-methylphenyl]}-6-hydroxy-3*H*-xanthen-3-one Mono(2′,3′,4′,6′-tetra-*O*-acetyl-β-D-galactopyranoside) (21). To a solution of **18** (37.7 mg, 0.049 mmol) in methanol/water (1.5 mL:0.5 mL) 2 M aq. NaOH (1 mL, 2 mmol) was added. The mixture was stirred at 0 °C for 30 min and then neutralized with Amberlite IR-120 (H$^+$). The Amberlite IR-120 was filtered off, and the filtrate was evaporated. The residue was subjected to reversed-phase preparative TLC (RP18W) with acetonitrile/water (1:1) as the eluent to give **21** as an orange powder (15.1 mg, 53%). ^{1}H NMR (300 MHz, CD_3OD) δ 7.26 (d, 1H, J = 2.2 Hz), 7.11 (d, 1H, J = 8.5 Hz), 7.08 (d,1H, J = 9.6 Hz), 7.03 (d, 1H, J = 8.2 Hz), 7.02 (dd, 1H, J = 8.5 Hz, 2.2 Hz), 6.94 (d, 1H, J =2.3 Hz), 6.89 (dd, 1H, J = 8.2 Hz, 2.3 Hz), 6.53 (dd, 1H, J = 9.6 Hz, 2.0 Hz), 6.37 (d, 1H, J = 2.0 Hz), 4.01 (m, 2H), 5.00 (dd, 1H, J = 7.7 Hz, 2.6 Hz), 3.83 (d, 1H, J = 3.3 Hz), 3.82−3.64 (m, 4H), 3.53 (dd, 1H, J = 9.7 Hz, 3.3 Hz), 2.17 (m, 2H), 1.93 (s, 3H), 1.74 (m, 4H). HRMS (ESI$^+$): calcd for [M + Na]$^+$, 603.184 23; found, 603.182 42.

Synthesis of 9-{1-[4-(4-acetoxymethoxycarbonylbutyloxy)-2-methylphenyl]}-6-hydroxy-3*H*-xanthen-3-one Mono-β-D-galactopyranoside (22). To a solution of **21** (10 mg, 17.2 μmol) in methanol/acetonitrile (1 mL:2 mL) a solution of bromomethyl acetate (68.5 μL, 690 μmol) and *N*,*N*-diisopropylethylamine (22.3 μL, 130 μmol) in acetonitrile (2 mL) was added slowly. The mixture was stirred at room temperature under argon for 10 h and then concentrated under reduced pressure. The residue was purified by semipreparative reversed-phase HPLC using eluent A (100 mM triethylammonium acetate buffer, pH 6.5) and eluent B (acetonitrile) (A/B = 65/35) to give **22** as an orange powder (10.9 mg, 97%). ^{1}H NMR (300 MHz, CD_3OD) δ 7.28 (d, 1H, J = 2.2 Hz), 7.13−6.88 (m, 6H), 6.53 (dd, 1H, J = 9.7 Hz, 2.0 Hz), 6.38 (dd, 1H, J = 2.0 Hz), 5.65 (s, 2H), 4.02 (m, 2H), 5.01 (dd, 1H, J = 8.1 Hz, 2.8 Hz), 3.83 (d, 1H, J = 3.1 Hz), 3.79−3.65 (m, 4H), 3.53 (dd, 1H, J = 9.5 Hz, 3.6 Hz), 2.42 (m, 2H), 1.99 (s, 3H), 1.94 (s, 3H), 1.78 (m, 4H). HRMS (ESI$^+$): calcd for [M + Na]$^+$, 675.205 36; found, 675.203 59.

Synthesis of 9-{1-[4-(4-acetoxymethoxycarbonylbutyloxy)-2-methylphenyl]}-6-hydroxy-3*H*-xanthen-3-one (23). To a solution of **20** (2.8 mg, 6.7 μmol) in dimethylformamide (0.5 mL), a solution of bromomethyl acetate (6.8 μL, 69 μmol) and *N*,*N*-diisopropylethylamine (2.2 μL, 13 μmol) in dimethylformamide (0.5 mL) was added. The mixture was stirred at room temperature under argon overnight, then diluted with H_2O, and extracted with ethyl acetate. The combined organic layer was concentrated under reduced pressure. The residue was purified by semipreparative reversed-phase HPLC with a linear gradient of eluent A (100 mM triethylammonium acetate buffer, pH 6.5) and eluent B (acetonitrile) (initial, 70% A/30% B; final (20 min), 30% A/70% B) to give **23** as an orange powder (0.88 mg, 27%). ^{1}H NMR (300 MHz, CD_3OD): δ 7.11 (d, 1H, J = 8.3 Hz), 7.00−7.05 (m, 3H), 6.97 (dd, 1H, J = 8.3, 2.5 Hz), 6.59−6.64 (m, 4H), 5.48 (s, 2H), 4.11 (t, 2H, J = 5.3 Hz), 2.50 (t, 2H, J = 6.6 Hz), 2.07 (s, 3H), 2.02 (s, 3H), 1.90−1.84 (m, 4H). HRMS (ESI$^+$): calcd for [M + H]$^+$, 491.170 59; found, 491.174 93.

Synthesis of *m*-Methoxycarbonylmethoxytoluene (Bn($\underline{1}^{Me}$)). A mixture of *m*-cresol (3 g, 27.7 mmol), bromomethyl acetate (4.67 g, 30.5 mmol), and Cs_2CO_3 (18 g, 55.5 mmol) in DMF (100 mL) was stirred at room temperature under argon for 4 h. The inorganic precipitate was filtered off, and the filtrate was concentrated under reduced pressure. The residue was diluted with CH_2Cl_2 three times, washed with water and saturated aq. NaCl, dried over Na_2SO_4, and evaporated. The residue was chromatographed on silica gel with CH_2Cl_2 as the eluent to give **Bn($\underline{1}^{Me}$)** as a colorless clear oil (5 g, quant.). ^{1}H NMR (300 MHz, $CDCl_3$) δ 7.17 (t, 1H, J = 7.9 Hz), 6.79−6.84 (m, 1H), 6.73−6.76 (m, 1H), 6.72−6.68 (m, 1H), 4.62 (s, 2H), 3.79 (d, 3H, J = 4.58 Hz), 2.33 (s, 3H); ^{13}C NMR (75 MHz, $CDCl_3$) δ 169.47, 157.72, 139.64, 129.22, 122.57, 115.49, 111.28, 65.19, 52.14, 21.41. MS (EI): *m*/*z* 180 (M$^+$).

Synthesis of *m*-Methoxycarbonylmethoxyanisole (Bn($\underline{2}^{Me}$)). A mixture of *m*-methoxyphenol (1.72 g, 13.8 mmol), bromomethyl acetate (2.34 g, 15.2 mmol), and Cs_2CO_3 (9 g, 27 mmol) in DMF (100 mL) was stirred at room temperature under argon for 4 h. The inorganic precipitate was filtered off, and the filtrate was concentrated under reduced pressure. The residue was diluted with CH_2Cl_2 three times, washed with water and saturated aq. NaCl, dried over Na_2SO_4, and evaporated. The residue was chromatographed on silica gel with CH_2Cl_2 as the eluent to give **Bn($\underline{2}^{Me}$)** as a colorless clear oil (2.66 g, 98%). ^{1}H NMR (300 MHz, $CDCl_3$): δ 7.18 (t, 1H, J = 8.1 Hz), 6.57−6.53 (m, 1H), 6.50−6.45 (m, 2H), 4.61 (s, 2H), 3.80 (s, 3H), 3.78 (s, 3H).; ^{13}C NMR (75 MHz, $CDCl_3$): δ 169.29, 160.83, 158.92, 129.95, 107.45, 106.30, 101.30, 65.24, 55.24, 52.19; MS (EI): *m*/*z* 196 (M$^+$).

Synthesis of *m*-methoxycarbonylbutyloxytoluene (Bn($\underline{3}^{Me}$)). A mixture of *m*-cresol (1 g, 9.2 mmol), 5-bromovaleric acid methyl ester (1.98 g, 10.1 mmol), and Cs_2CO_3 (6 g, 18.5 mmol) in DMF (50 mL) was stirred at room temperature under argon for 4 h. The inorganic precipitate was filtered off and the filtrate was concentrated under reduced pressure. The residue was diluted with CH_2Cl_2 three times, washed with water and saturated aq. NaCl, dried over Na_2SO_4, and evaporated. The residue was chromatographed on silica gel with CH_2Cl_2 as the eluent to give **Bn($\underline{3}^{Me}$)** as a colorless clear oil (2 g, 99%). ^{1}H NMR (300 MHz, $CDCl_3$) δ 7.16 (t, 1H, J = 7.7 Hz), 6.74−6.78 (m, 1H), 6.68−6.74 (m, 2H), 3.96 (t, 2H, J = 5.9 Hz), 3.68 (s, 3H), 2.41 (t, 2H, J = 7.0 Hz), 2.33 (s, 3H), 1.86−1.80 (m, 4H). ^{13}CNMR (75 MHz, $CDCl_3$) 173.82, 158.89, 139.34, 129.08, 121.36, 115.27, 111.24, 67.08, 51.43, 33.61, 28.65, 21.60, 21.43. MS (EI): *m*/*z* 222 (M$^+$).

Acknowledgment. This study was supported in part by the Intramural Research Program of the NIH, National Cancer Institute, Center for Cancer Research, a Grant-in-Aid for Creative Scientific Research (No. 13NP0401) to Y.U., research grants (Grant Nos. 18038008, 16651106, and 16689002) to Y.U., and a grant for the Advanced and Innovational Research Program in Life Sciences to T.N., research grants (grant Nos. 16370071 and 16659003) to T.N. from the Ministry of Education, Culture, Sports, Science and Technology of the Japanese Government, and by grants from Hoansha Foundation to T.N. and from Kowa Life Science Foundation to Y.U.

Supporting Information Available: Three figures in pdf file. This material is available free of charge via the Internet at http://pubs.acs.org.

JA067710A